

Quasiparticle band structure based on a generalized Kohn-Sham scheme

F. Fuchs,* J. Furthmüller, and F. Bechstedt

*Institut für Festkörperteorie und -optik, Friedrich-Schiller-Universität,
Max-Wien-Platz 1, D 07743 Jena, Germany*

M. Shishkin, G. Kresse

*Institut für Materialphysik and Center for Computational Materials Science,
Universität Wien, A 1090 Wien, Austria*

(Dated: December 2, 2024)

Abstract

We present the first comparative all-electron (AE) study of generalized Kohn-Sham schemes (gKS) with explicit focus on their suitability as starting point for the calculation of quasiparticle (QP) states. The gKS and QP band structures for the cubic semiconductors Si, ZnO and InN based on the LDA, sX, HSE, PBE0, and HF functionals for exchange and correlation (XC) are compared. We show that the QP energies resulting from a perturbative treatment of the GW self-energy are, with the exception of HF, rather independent of the start functional. We especially suggest the use of a gKS scheme as a starting point for solids with a wrong energetical ordering of the bands within local approximations for XC.

PACS numbers: 71.15.Mb, 71.15.Qe, 71.20.Nr

*Electronic address: fuchs@ifto.physik.uni-jena.de

Density Functional Theory (DFT) [1, 2] has become the most successful method for condensed matter calculations. This success is largely due to the treatment of the exchange and correlation (XC) energy in local density (LDA) or generalized gradient (GGA) approximation. However, the underlying Kohn-Sham (KS) formalism fails in the prediction of electronic excitation energies of semiconductors and insulators [3]. A significant step forward to correct excitation energies was achieved when the first *ab initio* calculations of quasiparticle (QP) states were performed [4, 5]. They are based on Hedin's GW approximation (GWA) for the XC self-energy [6] and a perturbative treatment of the difference to the XC potential used in the KS equation. For many nonmetals, such as the semiconductor silicon (Si), the method works well with an accuracy of 0.1 eV for their QP gaps [3], if the Green's function G is described by one pole at the KS, or better, at the QP energy. However, for systems with a wrong energetical ordering of the KS bands the perturbation-theory has to be overcome [7]. Examples are semiconductors with a negative fundamental gap in DFT-LDA or -GGA (e.g. InN [8] and references therein).

Besides the KS approach itself, the origin of the band gap problem is related to the semi-local approximation (LDA/GGA), which introduces an unphysical self-interaction and lacks a derivative discontinuity. Given an exact realisation of DFT the latter one would fully account for the difference of the KS and the QP gap of a nonmetal [9, 10]. The effects caused by the spurious self-interaction can be studied using self-interaction-free exact exchange (EXX) potentials [11], which are special realizations of an optimized effective potential (OEP) methods, and therefore also referenced to as OEPx [12]. Indeed, for *sp* semiconductors the EXX band structures were found to compare much better to the experiment than the LDA ones [11], even though the success is reduced for insulators [13] and upon the use of an all-electron (AE) method [14], or inclusion of correlation in the OEP framework [15]. A conceptually different way to attenuate the band gap problem is the use of a generalized Kohn-Sham (gKS) scheme [16]. In this framework the screened-exchange (sX) approximation uses a statically screened Coulomb kernel instead of the bare kernel in the Hartree-Fock (HF) exchange [16] and, with it, resembles the screened-exchange (SEX) contribution to the XC self-energy in the GWA [5, 6]. Other hybrid functionals such as those following the suggestions of Adamo and Barone (PBE0) [17] or Heyd, Scuseria, and Ernzerhof (HSE) [18] combine parts of bare or screened exchange with an explicit density functional. The gKS eigenvalues of the aforementioned functionals are usually in much better agreement with the experiment than the LDA/GGA ones. Therefore the gKS solutions are supposed to be superior starting points for a QP correction.

In this Letter we report a systematic study of QP energies calculated from GW corrections to the results of gKS schemes. To this end, we perform gKS and GW calculations for Si, InN, and ZnO using the gKS functionals sX, HSE, PBE0, and HF. The results are compared to those of the standard KS approach based on an LDA functional. We show that, compared to the latter one, gKS functionals give equivalently good or, in the case of subtle materials, much better starting points for a QP calculation. Furthermore, in this case the QP results are found to be rather independent of the actual starting functional. As test quantities we consider the fundamental gaps and shallow core d band binding energies which, for the standard LDA+GW treatment, fail with an underestimated or even zero gap for ZnO and InN and underbound d states in both cases.

The calculations are performed within the projector-augmented-wave (PAW) method [19] as implemented in the Vienna *Ab initio* Simulation Package [20]. In the framework of PAW the exact nodal structure of the one-electron valence wavefunctions is accounted for, while the plane-wave cutoff in the expansion of the pseudo wavefunctions can be significantly reduced compared to norm-conserving pseudopotentials. The PAW method can also be applied in GWA calculations yielding results comparable to other all-electron methods [21, 22, 23]. In addition, as other all-electron methods, the PAW method allows for the evaluation of the non-local core-valence exchange and thereby to go beyond the LDA treatment of core-valence exchange and correlation, inherent in the common pseudopotential approaches. This was found to be important for the gap [23, 24, 25] especially for semiconductors with semicore d states [12, 14].

For simplicity, we study here only the respective diamond or zinc-blende polytypes of the materials mentioned above. The calculations are performed at the experimental lattice constants and a common plane wave cutoff of 400 eV. For the Brillouin zone integrations a Γ -centered $8 \times 8 \times 8$ Monkhorst-Pack k -point mesh is used, resulting in a convergence better than 50 meV for the electronic levels. The PAW datasets used for In and Zn include partial waves up to $l = 2$ in order to guarantee an accurate treatment of the In $4d$ and Zn $3d$ electrons as valence states. An accurate calculation of the dielectric response functions from gKS schemes requires to include selfconsistent field effects from the non-local exchange operator, which makes a direct evaluation of $W(\mathbf{x}, \mathbf{x}'; \epsilon)$ exceedingly time consuming [26]. Thus for the valence electrons, the GW self-energy operator $\Sigma(\mathbf{x}, \mathbf{x}'; \epsilon)$ is constructed from the pseudo wave-functions as in Ref. [27] using a model dielectric function together with a plasmon-pole approximation for the dynamical contribution [28]. The residual PAW one center terms include only high spatial frequencies and are therefore approximated by the corresponding HF exchange contribution [23]. For the static fixed-ion dielectric

TABLE I: Parameters of the gKS exchange functionals used.

Functional	α	<i>sr</i> Coulomb kernel	μ [\AA^{-1}]
LDA	0.00	$1/ \mathbf{x} $	-
sX	1.00	$\exp(-\mu \mathbf{x})/ \mathbf{x} $	1.55
HSE	0.25	$\text{erfc}(\mu \mathbf{x})/ \mathbf{x} $	0.3
PBE0	0.25	$1/ \mathbf{x} $	-
HF	1.00	$1/ \mathbf{x} $	-

constant ϵ_∞ , which enters the model dielectric function, the experimental values [8, 29, 30] of 11.7, 7.9 and 3.7 are used for Si, InN, and ZnO respectively.

The XC contribution from the core-valence (cv) interaction can be estimated from the LDA or the HF approximation, where the latter one is expected to be more reliable, since the GW self-energy approaches the bare Fock exchange operator in the shorth wave-length regime (i.e. at large binding energies). Here we use the HF approximation – for the sake of consistency – in all GW and gKS calculations. Only the LDA calculations feature cv-XC on the LDA level.

Since, the actual implementation of the gKS schemes differs somewhat from the ones found in the original papers we will briefly summarize the keypoints here. We split the gKS XC energy into the form:

$$E_{XC}^{gKS} = E_{XC}^{LDA} + \alpha \left[E_X^{sr}(\mu) - E_X^{LDA,sr}(\mu) \right], \quad (1)$$

i.e. a short range non-local exchange term is subtracted and treated exactly resulting in a non-local (screened) exchange potential. The superscript *LDA* indicates that the respective quantity is evaluated in some (quasi)local approximation, while E_X^{sr} corresponds to one of the (screened) Coulomb kernels given in Table I. The weight α of the short range part and the inverse screening length μ are also listed in this table. For simplicity, in the case of sX, the inverse screening length μ corresponding to the Thomas-Fermi wavevector was chosen material independent $k_{TF} = 1.55 \text{ \AA}^{-1}$ here. This value corresponds roughly to 70% of the average k_{TF} estimated from the density of valence *sp* electrons. Another important detail concerns the implementation of the LDA part in the sX case. Seidl et al. [16] suggest the use of a global enhancement factor z , while in the spirit of LDA the VASP implementation features a local enhancement factor $\tilde{z} = k_{TF}/k_F$, where the Fermi wavevector k_F depends on the local density $n(\mathbf{x})$.

TABLE II: Generalized KS band gaps E_g^{gKS} , valence-band widths $W_{\text{val}}^{\text{gKS}}$, and average d -band binding energies E_d^{gKS} (with respect to the valence-band maximum) calculated for cubic Si, ZnO, and InN. For Si previous theoretical results [16, 18, 27] are given in parenthesis. Experimental values are from data collections in Refs. [8, 27, 29, 31, 32, 33]. In the case of InN and ZnO they refer, however, to the wurtzite polytype. All values are given in eV.

	Energy	LDA	sX	HSE	PBE0	HF	Exp.
Si	E_g^{gKS}	0.47	0.96	0.99	1.81	6.45	1.17
	(indirect)	(0.44)	(1.55)	(1.28)		(6.43)	
	E_g^{gKS}	2.52	3.25	3.19	4.03	9.13	3.4
	(direct)	(2.43)	(3.37)			(9.27)	
	$W_{\text{val}}^{\text{gKS}}$	11.96	13.45	13.21	13.44	17.01	12.5
		(12.08)	(12.47)				
ZnO	E_g^{gKS}	0.57	2.88	2.30	3.24	10.91	3.44
	E_d^{gKS}	4.9	8.0	7.9	8.0	9.2	7.0-8.8
InN	E_g^{gKS}	-0.35	0.59	0.38	1.17	7.20	0.7
	E_d^{gKS}	13.0	16.9	17.2	17.4	18.6	16.0-16.9

The results of the gKS calculations are summarized in Table II together with previous experimental and theoretical results. The gaps and valence band widths calculated for Si are in rather good agreement with published theoretical data. The differences mainly arise from the different implementation as discussed above. We notice an increase of the computed gaps when going from the local density approximation to a truly non-local XC functional. This can be attributed to the reduction of the spurious self-interaction found in LDA, the inclusion of a derivative discontinuity in the XC functional [9, 10, 16] and the, in comparison to LDA, enhanced core-valence exchange. Furthermore, we observe the tendency for the direct gaps to increase from LDA over HSE, sX and PBE0 to the HF values. In the following we refer to the d band binding energy as the position of the respective maximum in the DOS instead of the averaged Γ point values. For ZnO and InN, we observe a significant increase of the d band binding energies with respect to the LDA improving the results towards the experiment. Moreover, the d band binding energies are found to vary only little with the gKS functional.

In comparison to the experiment the gKS functional, with exception of HF, generally perform better than standard DFT-LDA for the gaps as well as the binding energies of the d electrons. There is another important fact to note for InN. All gKS functionals are found to yield the correct ordering of states at the zone center, in contrast to LDA findings [8] which give a negative sp gap. This is essential for the QP description, since a correct energetical ordering of the single-particle states is an inevitable prerequisite for a perturbative treatment of the GW corrections [3, 34]

The correct energetical ordering and the relatively small deviations of the gKS eigenvalues from measured excitation energies suggest that the QP energies $\varepsilon_\lambda^{\text{QP}}$ can be calculated to first order in $(\varepsilon_\lambda^{\text{QP}} - \varepsilon_\lambda^{\text{gKS}})$ as

$$\varepsilon_\lambda^{\text{QP}} = \varepsilon_\lambda^{\text{gKS}} + \frac{1}{1 - \beta_\lambda} \Delta_{\lambda\lambda}(\varepsilon_\lambda^{\text{gKS}}), \quad \beta_\lambda = \left. \frac{\partial \Delta_{\lambda\lambda}(\varepsilon)}{\partial \varepsilon} \right|_{\varepsilon_\lambda^{\text{gKS}}}, \quad (2)$$

with the matrix element

$$\Delta_{\lambda\lambda'}(\varepsilon) = \langle \psi_\lambda^{\text{gKS}} | \hat{\Sigma}(\varepsilon) - \hat{V}_{XC} | \psi_{\lambda'}^{\text{gKS}} \rangle \quad (3)$$

of the perturbation operator. It is noted, that V_{XC} is a non-local potential for gKS schemes. Non-diagonal elements $\Delta_{\lambda\lambda'}(\lambda \neq \lambda')$ and hence an update of the QP eigenfunctions can be neglected. According to (2) the diagonal element $\Delta_{\lambda\lambda}$ times the renormalization factor $(1 - \beta_\lambda)^{-1}$ defines the QP shift for a certain gKS state λ . For InN and ZnO these shifts are plotted in Fig. 1 versus the gKS eigenenergy. The QP shifts for the HF functional are not shown, since the absolute values of the negative (positive) shifts for the empty (occupied) states are too large. For InN [Fig. 1(a)] the QP shifts for the upper valence bands and the conduction bands show a rather weak dispersion with the eigenstate. They may be approximated by scissor operators for occupied and empty states whose absolute values depend on the used gKS functional LDA, sX, HSE, or PBE0. Only for the lowest In4*d*- and N2*s*-derived bands at gKS energies below -10 eV the QP shifts show a dispersion. This is most pronounced in the LDA case and reduces significantly upon the use of a gKS functional. Interestingly, the sX starting point leads to the weakest variation of the QP shifts in all energy regimes considered. This might be attributed to the conceptual proximity of sX to the SEX term in the GW self-energy which dominates the state dependence of the QP shifts. The findings for ZnO (Fig. 1b) are similar. However, since the Zn3*d* states are bound much weaker, the effect of the pd repulsion is stronger than in InN resulting in a stronger influence of the d electrons on the uppermost occupied states and hence the corresponding QP shifts.

FIG. 1: (Color online) Quasiparticle shifts versus gKS eigenvalues for InN (a) and ZnO (b). The valence-band maximum (VBM) and the conduction-band minimum (CBM) are taken as energy zeros occupied and empty states, respectively. Results for four different starting gKS band structures are shown. Diamonds: LDA, (red) dots: sX, (blue) triangles: HSE, and (green) squares.

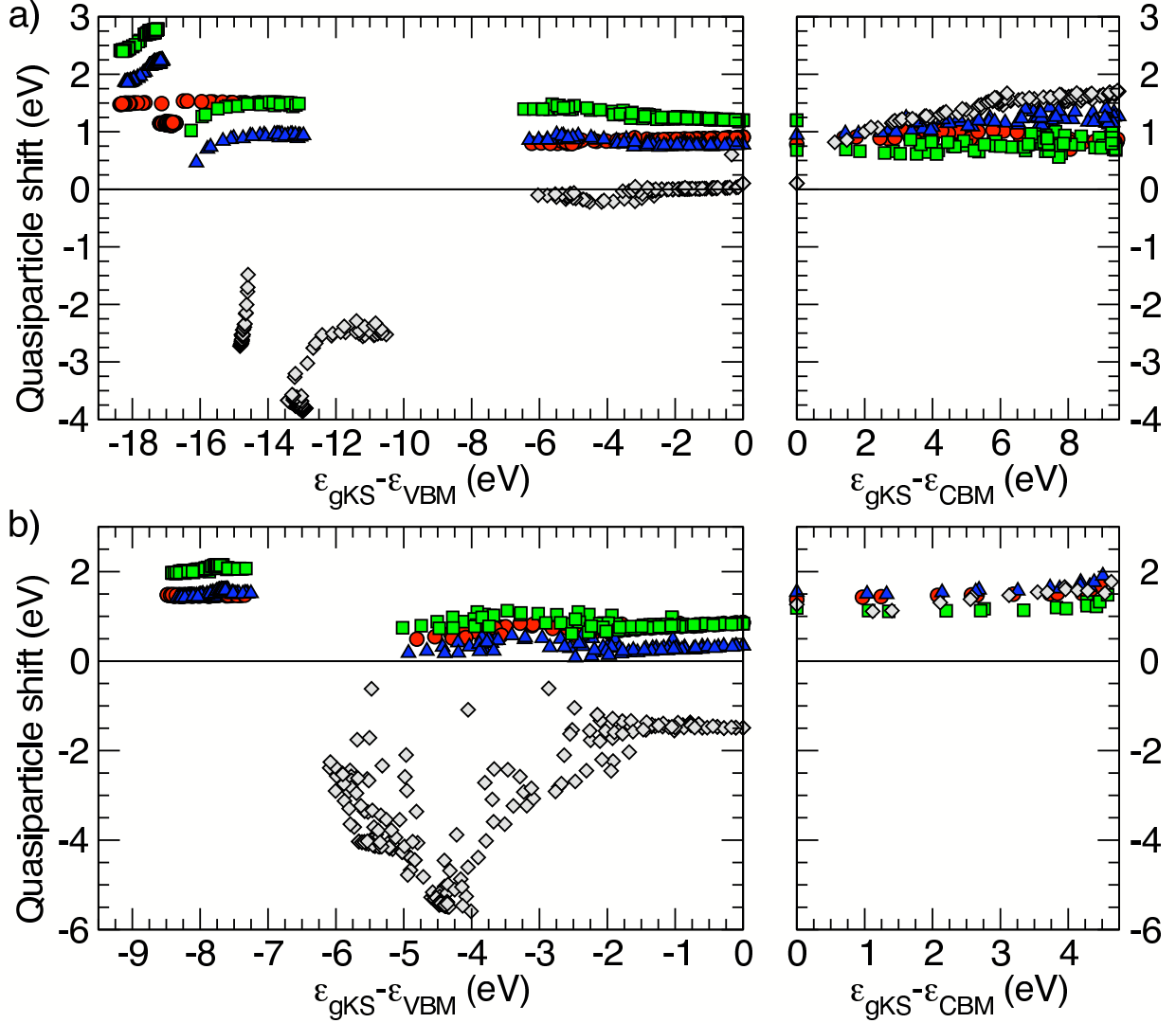


Table III shows the results of the gKS+GW calculations for the gaps, band widths, and d -electron binding energies. Despite the large scatter in the gKS gaps in Table II, the gKS+GW gaps for Si but also for InN and ZnO are almost the same, with exception of the combination of HF+GW. The deviations from the average are about 0.1 eV or smaller. Clearly, this is a consequence of the validity of the perturbative QP treatment. In contrast, starting from HF, the differences between $\epsilon_{\lambda}^{\text{QP}}$ and $\epsilon_{\lambda}^{\text{HF}}$ are so large that the perturbative treatment in (3) becomes invalid. The QP energies shown in Table III have a physical meaning as measurable quantities, in contrast to the LDA or gKS

energies. Indeed the agreement with the experimental values also shown in this table is excellent, considering that in the case of ZnO and InN a gap lowering of about 0.2 eV of the zinc-blende polymorph with respect to the wurtzite value should be taken into account [8, 12]. The LDA+GW gap for Si also compares well with the experiment, but not for InN and ZnO. For InN this is due to the wrong band ordering that renders the LDA a bad starting point. For ZnO the overestimation of the gap at first seems to be in conflict with recent results [12]. However, it is largely caused by the different treatment of the core-valence XC interaction and the unphysically high d -content of the VBM found in LDA. Upon a LDA treatment of cv-XC in the GW calculation, comparable to [12], the respective LDA+GW gap narrows to a value of 2.52 eV. Furthermore, the LDA+GW QP gap of Ref. [12] is influenced by an overscreening from the dielectric function calculated upon LDA eigenvalues, which was identified as the main source of error in another all-electron LDA+GW calculation for ZnO [35] resulting in a QP gap of 2.44 eV. It is also interesting to compare the present results with those of the OEP_x+GW method of Ref. 12. The gap calculated there amounts to 3.1 eV which is also in very good agreement with the gap expected for cubic ZnO, but seems a little underestimated. The present QP corrected sX , HSE and PBE0 results show the opposite tendency and slightly overestimate the gap.

Compared to the gaps, the d band binding energies calculated for InN and ZnO show a stronger variation with the starting XC functional. Nevertheless, the agreement of the calculated values with experimental ones (Table III) is good for InN. For ZnO the picture is less clear, although, here the comparison with experiment is also hampered by the remarkable scatter in the measured values. In any case, despite the large improvements due to the other starting functionals, the predictive power for the energy positions of the semicore d -bands is reduced with respect to that for the gaps.

In conclusion, we have presented QP calculations starting from gKS schemes with a variety of XC functionals LDA, sX , HSE, PBE0, and HF for the cubic semiconductors Si, InN, and ZnO. We found that the gKS schemes that take into account a screened or parts of a non-local (screened) exchange (sX , HSE, PBE0) potential give rise to eigenvalues much closer to the experimental excitation energies. Furthermore, in case that the perturbative treatment is valid, the subsequently applied GW corrections are found to yield QP energies which are almost independent of the actual starting functional and compare well with the experiment (especially for gaps). The reasons for these particularly vast improvements over the LDA are the comparably small differences of the gKS and the QP bandstructure, including the correct ordering of states. The latter one is important

TABLE III: Direct (d) and indirect (i) QP band gaps , valence band widths, and average d -band binding energies calculated upon the respective gKS bandstructures for Si, ZnO, and InN bulk. All values are given in eV. Experimental results are also given for comparison.

	Energy	LDA	sX	HSE	PBE0	HF	Exp.
Si	$E_g^{\text{QP}}(\text{i})$	1.00	1.17	1.16	1.32	2.32	1.17
	$E_g^{\text{QP}}(\text{d})$	3.22	3.41	3.38	3.55	4.62	3.4
	$W_{\text{val}}^{\text{QP}}$	12.9	13.1	13.1	13.2	13.8	12.5
ZnO	E_g^{QP}	4.01	3.38	3.49	3.59	4.26	3.44
	E_d^{QP}	8.5	7.4	6.7	6.7	8.2	7.0-8.8
InN	E_g^{QP}	0.00	0.46	0.55	0.65	1.31	0.7
	E_d^{QP}	16.9	16.7	15.9	15.9	17.5	16.0-16.9

especially for solids such as InN for which the LDA XC functional fails with a wrong ordering of the band edges. The use of gKS functions as starting points for GW calculations instead of the use of LDA or GGA seems a way to avoid the self-consistent inclusion of nondiagonal elements of the self-energy operator (cf. equ. (3)) and, hence, may help to make possible QP calculations also for complex systems.

Financial support by the Deutsche Forschungsgemeinschaft (Project No. Be 1346/18-1) and the European Community in the framework of the network of excellence NANOQUANTA (Contract No. NMP4-CT-2004-500198) and the Austrian FWF is gratefully acknowledged.

-
- [1] P. Hohenberg and W. Kohn, Phys. Rev. **136**, B864 (1965).
 - [2] W. Kohn and L. Sham, Phys. Rev. **140**, A1133 (1964).
 - [3] W. Aulbur, L. Jönsson, and J. Wilkins, Solid State Phys. **54**, 1 (2000).
 - [4] R. W. Godby, M. Schlüter, and L. J. Sham, Phys. Rev. Lett. **56**, 2415 (1986).
 - [5] M. S. Hybertsen and S. G. Louie, Phys. Rev. Lett. **55**, 1418 (1985).
 - [6] L. Hedin, Phys. Rev. **139**, A796 (1965).
 - [7] O. Pulci, F. Bechstedt, G. Onida, R. Sole, and L. Reining, Phys. Rev. B **60**, 16758 (1999).

- [8] J. Furthmüller, P. H. Hahn, F. Fuchs, and F. Bechstedt, *Phys. Rev. B* **72**, 205106 (2005).
- [9] J. P. Perdew and M. Levy, *Phys. Rev. Lett.* **51**, 1884 (1983).
- [10] L. J. Sham and M. Schlüter, *Phys. Rev. Lett.* **51**, 1888 (1983).
- [11] M. Städele, J. A. Majewski, P. Vogl, and A. Görling, *Phys. Rev. Lett.* **79**, 2089 (1997).
- [12] P. Rinke, A. Qteish, Neugebauer, C. Freysoldt, and M. Scheffler, *New J. Phys.* **7**, 126 (2005).
- [13] R. Magyar, A. Fleszar, and E. Gross, *Phys. Rev. B* **69**, 045111 (2004).
- [14] S. Sharma, J. K. Dewhurst, and C. Ambrosch-Draxl, *Phys. Rev. Lett.* **95**, 136402 (2005).
- [15] M. Grüning, A. Marini, and A. Rubio, *J. Chem. Phys.* (submitted)
- [16] A. Seidl, A. Görling, P. Vogl, J. A. Majewski, and M. Levy, *Phys. Rev. B* **53**, 3764 (1996).
- [17] C. Adamo and V. Barone, *J. Chem. Phys.* **110**, 6158 (1999).
- [18] J. Heyd, G. E. Scuseria, and M. Ernzerhof, *J. Chem. Phys.* **118**, 8207 (2003).
- [19] G. Kresse and J. Joubert, *Phys. Rev. B* **59**, 1758 (1999).
- [20] G. Kresse and J. Furthmüller, *Comp. Mat. Science* **6**, 15 (1996).
- [21] B. Arnaud and M. Alouani, *Phys. Rev. B* **62**, 4464 (2000).
- [22] S. Lebègue, B. Arnaud, M. Alouani, and P. E. Bloechl, *Phys. Rev. B* **67**, 155208 (2003).
- [23] M. Shishkin and G. Kresse, *Phys. Rev. B* (submitted).
- [24] M. Rohlfing, P. Krüger, and J. Pollmann, *Phys. Rev. Lett.* **75**, 3489 (1995).
- [25] W. Ku and A. G. Egiluz, *Phys. Rev. Lett.* **89**, 126401 (2002).
- [26] J. Paier, M. Shishkin, G. Kresse, (unpublished).
- [27] J. Furthmüller, G. Cappellini, H.-C. Weissker, and F. Bechstedt, *Phys. Rev. B* **66**, 0450110 (2002).
- [28] F. Bechstedt, R. Del Sole, G. Cappellini, and L. Reining, *Solid State Communications* **84**, 765 (1992).
- [29] *Landold-Börnstein, Numerical Data and Functional Relationships in Science and Technology, New Series, Group III*, edited by K. H. Hellwege and O. Madelung (Springer, Berlin, 1982), Vol. 17 and 22.
- [30] N. Ashkenov *et al.*, *Journal of Applied Physics* **93**, 126 (2003).
- [31] L. F. J. Piper *et al.*, *Phys. Rev. B* **72**, 245319 (2005).
- [32] L. Ley *et al.*, *Phys. Rev. B* **9**, 600 (1974).
- [33] R. Girard *et al.*, *Surface Science* **373**, 409 (1997).
- [34] T. Kotani and M. van Schilfgaarde, *Solid State Commun.* **121**, 461 (2002).
- [35] M. Usuda, N. Hamada, T. Kotani, and M. van Schilfgaarde, *Phys. Rev. B* **66**, 125101 (2002).